

# AUGMENTED LAGRANGIAN FINITE-ELEMENTS FOR PLATE CONTACT PROBLEMS

FERDINANDO AURICCHIO

*Dipartimento di Ingegneria Civile, Universita' di Roma 'Tor Vergata', Via della Ricerca Scientifica, 00133, Roma, Italy*

ELIO SACCO

*Dipartimento di Ingegneria Industriale, Universita' di Cassino, Via Zamasch 43, 03043, Cassino, Italy*

## SUMMARY

The present work investigates the unilateral frictionless contact between a plate and a rigid obstacle. Two sets of problems are studied: a plate constrained through unilateral edge supports and a plate seating in its undeformed configuration at a given distance from a rigid support. The attention is concentrated on two augmented Lagrangian formulations. The algorithmic implementation within a finite-element scheme is presented and discussed. The importance of using appropriate plate elements for the discretization of the structure is stressed. New gap elements compatible with a robust plate element are derived. Computational aspects are emphasized. A simple and effective numerical integration for the determination of the gap stiffnesses in partial contact with the support is proposed. Numerical results are carried out and compared with analytical solutions. The convergence to the solution of the perfectly constrained problem is numerically investigated. The inadequacy of the penalty method and the satisfactory performance obtained from only one augmented Lagrangian procedure are emphasized.

KEY WORDS: finite elements; plate; contact; augmented Lagrangian

## 1. INTRODUCTION

Unilateral contact problems are governed by inequalities. This class of problems can be cast in proper variational formulations, which allow the use of convex analysis tools.<sup>1,2</sup> Furthermore, variational formulations are particularly convenient if the goal is to perform numerical simulations, for examples by finite-element techniques.

Unilateral problems have been numerically solved within the penalty method<sup>3–5</sup> which regularizes the non-smooth constraint of the unilateral contact. In the last years augmented Lagrangian formulations have been employed more and more frequently for the treatment of constrained problems. Based on the Uzawa algorithm,<sup>6,7</sup> augmented Lagrangian schemes can be interpreted as iterative penalty methods and appear to be very effective in many applications. In particular, augmented Lagrangian formulations have been adopted in unilateral contact problems, including friction effects, for instance in References 8–13.

One of the most common contact problems deals with the unilateral contact between an elastic plate and rigid or elastic obstacles. For such structural problems, friction effects are generally neglected. In the literature, it appears that the most investigated cases, via the finite-element method, concern the contact of flat structures with elastic bodies. For instance, the unilateral contact between a plate and a homogeneous half-space is studied in References 14–16; the dynamics of a plate

resting on a Pasternak two-parameter foundation is investigated in Reference 17; the case of a Winkler foundation is considered in References 18 and 19; the unilateral contact, including the friction effects, between two elastic plates is studied in Reference 20. Thus, to the best of the authors' knowledge, there is a lack of studies for the case of plates in contact with rigid supports. Furthermore, the use of augmented Lagrangian schemes seems to have been partially overlooked for the solution of plate contact problems within finite-element schemes.

Plate structures are often modelled by a first-order shear deformation theory, which takes into account the primary effects of the shear deformation. In such a case, the use of inappropriate plate elements may induce numerical pathologies. As an example, Lagrangian isoparametric displacement-based elements<sup>21,22</sup> are simple to code and seem to be effective in many applications if selective integration formulas are adopted (to avoid the so-called *locking*).<sup>23</sup> However, the selective integration technique may introduce zero-energy modes,<sup>24</sup> which are possibly excited during the analysis of contact problems; in these cases the convergence may be extremely difficult to reach.<sup>18</sup> As a consequence, more effective and reliable elements must be used for the analysis of plate contact problems. Recently a new quadrilateral plate element has been proposed by Auricchio and Taylor.<sup>25</sup> The interpolation scheme adopted is such that the transverse displacement is linked to the nodal rotations, while the rotational field is enriched with bubble functions. The element is locking-free and performs well.

The present work focuses on field and edge contact problems between moderately thick plates and rigid supports. Two augmented Lagrangian functionals available in the literature are specialized to the problems investigated herein; their ability in enforcing properly the contact conditions in terms of displacement and pressure is carefully assessed. The four- and the nine-node Lagrangian isoparametric displacement-based plate finite-elements are reviewed together with their compatible gap elements; the relative numerical pathologies are highlighted. New gap elements compatible with the plate element based on a linked interpolation are derived and adopted for the solution of several contact problems. Computational aspects are emphasized. An efficient technique for the integration of the gap stiffness is introduced. Numerical results are compared with analytical solutions to show the performances of the considered formulations.

## 2. FORMULATION OF THE PROBLEM

In this section the unilateral frictionless contact problem between a moderately thick plate and a rigid support is formulated. The analysis is framed within a small deformation theory.

### 2.1. Moderately thick plates

A first-order shear deformation theory is adopted herein to model the response of moderately thick plates; the theory includes both bending deformation and the primary effects of transverse shear deformation<sup>26</sup> and follows in many fundamental aspects the ones proposed by Reissner<sup>27</sup> and Mindlin.<sup>28</sup> A *plate* is a flat body, occupying the domain

$$\Omega = \left\{ (x, y, z) \in \mathbb{R}^3 \mid z \in \left[ -\frac{h}{2}, +\frac{h}{2} \right], (x, y) \in \mathcal{A} \subset \mathbb{R}^2 \right\} \quad (1)$$

where the plane  $z = 0$  coincides with the middle surface of the undeformed plate and the transverse dimension, or *thickness*  $h$ , is smaller than the other two dimensions. Furthermore, the loading is

restricted to be in the direction normal to the middle surface. The displacements along the  $x$ ,  $y$  and  $z$  axes are indicated respectively by  $u$ ,  $v$  and  $w$  and are assumed in the form

$$\begin{aligned} u(x, y, z) &= z\theta_y(x, y) \\ v(x, y, z) &= -z\theta_x(x, y) \\ w(x, y, z) &= w(x, y) \end{aligned} \quad (2)$$

where  $\theta_x$  and  $\theta_y$  are the rotations of the transverse line elements (initially perpendicular to the mid-surface) about the  $x$  and  $y$  axes. The basic kinematic ingredients are the curvature,  $\mathbf{K}$ , and the shear strain,  $\mathbf{\Gamma}$ , defined as

$$\mathbf{K} = \mathbf{L}\boldsymbol{\theta}, \quad \mathbf{\Gamma} = [\mathbf{e}\boldsymbol{\theta} + \nabla w] \quad (3)$$

where

$$\mathbf{L} = \begin{bmatrix} \mathbf{0} & \frac{\partial}{\partial x} \\ -\frac{\partial}{\partial y} & \mathbf{0} \\ -\frac{\partial}{\partial x} & \frac{\partial}{\partial y} \end{bmatrix}, \quad \boldsymbol{\theta} = \begin{Bmatrix} \theta_x \\ \theta_y \end{Bmatrix}, \quad \mathbf{e} = \begin{bmatrix} 0 & 1 \\ -1 & 0 \end{bmatrix}, \quad \nabla = \begin{Bmatrix} \frac{\partial}{\partial x} \\ \frac{\partial}{\partial y} \end{Bmatrix} \quad (4)$$

Integration of the stress components through the thickness defines the plate stress resultants per unit length:

$$\mathbf{M} = \begin{Bmatrix} M_x \\ M_y \\ M_{xy} \end{Bmatrix} = \int_{-h/2}^{h/2} \begin{Bmatrix} \sigma_x \\ \sigma_y \\ \tau_{xy} \end{Bmatrix} dz, \quad \mathbf{S} = \begin{Bmatrix} S_x \\ S_y \end{Bmatrix} = \int_{-h/2}^{h/2} \begin{Bmatrix} \tau_{xz} \\ \tau_{yz} \end{Bmatrix} dz \quad (5)$$

Assuming the material to be homogeneous, linearly elastic and isotropic, the plate constitutive relation may be written in terms of the stress resultants and the dual kinematical variables as

$$\begin{Bmatrix} \mathbf{M} \\ \mathbf{S} \end{Bmatrix} = \begin{bmatrix} \mathbf{D}_B & \mathbf{0} \\ \mathbf{0} & \mathbf{D}_S \end{bmatrix} \begin{Bmatrix} \mathbf{K} \\ \mathbf{\Gamma} \end{Bmatrix} \quad (6)$$

where

$$\mathbf{D}_B = D \begin{bmatrix} 1 & \nu & 0 \\ \nu & 1 & 0 \\ 0 & 0 & \frac{1}{2}(1-\nu) \end{bmatrix}, \quad D = \frac{Eh^3}{12(1-\nu^2)} \quad (7)$$

$$\mathbf{D}_S = kGh \begin{bmatrix} 1 & 0 \\ 0 & 1 \end{bmatrix}, \quad G = \frac{E}{2(1+\nu)} \quad (8)$$

with  $E$  the Young's modulus,  $\nu$  the Poisson's ratio and  $k$  the shear factor (in the following set equal to 5/6).

## 2.2. Contact problem

The plate may be subjected to field and boundary constraints, due to possible unilateral frictionless contacts. The field constraint expresses the presence of a rigid obstacle, seating at a fixed

gap distance  $g$  from the undeformed plate bottom plane ( $z = h/2$ ). Accordingly, the transversal displacement  $w$  must satisfy the inequality

$$w - g \leq 0 \quad \text{in } \mathcal{A} \quad (9)$$

The boundary constraint expresses the possibility of unilateral contact along a part  $\partial_2 \mathcal{A}$  of the mid-plane boundary  $\partial \mathcal{A}$ . Accordingly,

$$w \leq 0 \quad \text{on } \partial_2 \mathcal{A} \quad (10)$$

Classical mixed boundary conditions are imposed on the remaining part of the boundary  $\partial_1 \mathcal{A} = \partial \mathcal{A} \setminus \partial_2 \mathcal{A}$ , i.e. displacements or forces are specified.

### 3. VARIATIONAL FORMULATION

In this section variational formulations of the previously addressed unilateral frictionless contact problem are introduced. In particular, the attention is concentrated on two augmented Lagrangian schemes.

The plate model can be cast in a variational formulation, introducing the following *mixed* functional:<sup>25</sup>

$$\begin{aligned} \Pi(w, \boldsymbol{\theta}, \mathbf{S}) = & \frac{1}{2} \int_{\mathcal{A}} [\mathbf{K}^T(\boldsymbol{\theta}) \mathbf{D}_B \mathbf{K}(\boldsymbol{\theta})] dA \\ & - \frac{1}{2} \int_{\mathcal{A}} [\mathbf{S}^T \mathbf{D}_S^{-1} \mathbf{S}] dA + \int_{\mathcal{A}} [\mathbf{S}^T (\nabla w + \mathbf{e}\boldsymbol{\theta})] dA + \Pi_{\text{ext}} \end{aligned} \quad (11)$$

where  $\Pi_{\text{ext}}$  is the load potential. Note that when the shear energy is set equal to zero (i.e.  $\mathbf{S}^T \mathbf{D}_S^{-1} \mathbf{S} = \mathbf{0}$ ), the shear resultant  $\mathbf{S}$  is the Lagrange multiplier of the constraint  $\nabla w + \mathbf{e}\boldsymbol{\theta} = \mathbf{0}$ . Thus, the classical Kirchhoff–Love plate theory is recovered.

The solution of the unilateral contact plate problem can be sought as the minimax condition of  $\Pi$  under the constraints (9) and (10). To avoid restrictions on the set of displacements, the Lagrange multiplier formulation can be considered:

$$\Lambda(w, \boldsymbol{\theta}, \mathbf{S}, r, p) = \Pi(w, \boldsymbol{\theta}, \mathbf{S}) - \int_{\mathcal{A}} [p(w - g)] dA - \int_{\partial_2 \mathcal{A}} r w ds \quad (12)$$

where the Lagrange multipliers  $p$  and  $r$  have the mechanical meaning of contact pressure per unit area acting on  $\mathcal{A}$  and contact pressure per unit length acting on  $\partial_2 \mathcal{A}$ , respectively. The minimax condition for  $\Lambda(w, \boldsymbol{\theta}, \mathbf{S}, r, p)$  subject to the constraints:

$$p \leq 0, \quad r \leq 0 \quad (13)$$

returns the complete solution of the elastostatic unilateral contact problem.

Augmented Lagrangian formulations can be obtained by augmenting the Lagrangian functional (12). In the case of linear constraints the augmented functional is usually obtained by adding to the Lagrangian the penalty terms corresponding to the constraints.<sup>6</sup> In the case of non-linear constraints, as for unilateral contact problems, the augmenting term is not unique and, in fact, different proposals can be found in the literature.

An augmented Lagrangian formulation for contact problems is described by Alart and Curnier.<sup>9</sup> The same formulation is presented in a more general mathematical framework by Ito and Kunisch.<sup>29</sup> In the following, a simple construction of the functional proposed in Reference 9 is presented.

Initially, the discussion is limited to the field constraint; the extension to the boundary constraint is simple and it is given in the final equation.

Let the surface  $\mathcal{A}$ , candidate to the unilateral contact, be split into two parts,  $\mathcal{A}_{nc}$  and  $\mathcal{A}_c$ , such that

$$\begin{aligned} w - g < 0 \quad \text{and} \quad p = 0 \quad \text{on} \quad \mathcal{A}_{nc} \\ w - g = 0 \quad \text{and} \quad p \leq 0 \quad \text{on} \quad \mathcal{A}_c \end{aligned}$$

Clearly,  $\mathcal{A} = \mathcal{A}_{nc} \cup \mathcal{A}_c$  with  $\mathcal{A}_{nc} \cap \mathcal{A}_c = \emptyset$ . Hence,  $\mathcal{A}_c$  represents the zone of the plate in contact and it is not known *a priori*. The saddle-point of the functional (12) can be computed considering the augmented Lagrangian:

$$\Lambda(w, \boldsymbol{\theta}, \mathbf{S}, r, p) + \frac{k_x}{2} \int_{\mathcal{A}_c} (w - g)^2 dA \tag{14}$$

since the last term is quadratic and zero in solution. The quantity  $k_x$  plays the role of a penalty parameter. The stationary condition for the functional (14) with respect to the variable  $w$  leads to the equation

$$\begin{aligned} 0 = \int_{\mathcal{A}} [\mathbf{S}^T \nabla \delta w] dA - \int_{\mathcal{A}_c} [p - k_x(w - g)] \delta w dA \\ - \int_{\mathcal{A}_{nc}} p \delta w dA + \delta_w \Pi_e \end{aligned} \tag{15}$$

Since  $p - k_x(w - g)$  in solution is non-positive on  $\mathcal{A}_c$ , then the functional (14) can be further augmented:

$$\Lambda(w, \boldsymbol{\theta}, \mathbf{S}, r, p) + \frac{k_x}{2} \int_{\mathcal{A}_c} (w - g)^2 dA - \frac{1}{2k_x} \int_{\mathcal{A}_c} \{[p - k_x(w - g)]^+\}^2 dA \tag{16}$$

A simple computation reveals that the whole augmentation term is quadratic and zero in solution also on  $\mathcal{A}_{nc}$ . Hence, taking into account the term relative to the boundary contact, the final augmented Lagrangian functional can be defined as

$$\begin{aligned} \Lambda_{aug}(w, \boldsymbol{\theta}, \mathbf{S}, r, p) = \Lambda(w, \boldsymbol{\theta}, \mathbf{S}, r, p) \\ + \frac{k_x}{2} \int_{\mathcal{A}} (w - g)^2 dA - \frac{1}{2k_x} \int_{\mathcal{A}} \{[p - k_x(w - g)]^+\}^2 dA \\ + \frac{k_\beta}{2} \int_{\partial_2 \mathcal{A}} w^2 ds - \frac{1}{2k_\beta} \int_{\partial_2 \mathcal{A}} [(r - k_\beta w)^+]^2 ds \end{aligned} \tag{17}$$

The solution state, obtained as the stationary point for the unconstrained functional (17), satisfies the equations

$$\begin{aligned} 0 = \int_{\mathcal{A}} [\mathbf{S}^T \nabla \delta w] dA - \int_{\mathcal{A}} [p - k_x(w - g)]^- \delta w dA \\ - \int_{\partial_2 \mathcal{A}} (r - k_\beta w)^- \delta w ds + \delta_w \Pi_e \end{aligned} \tag{18}$$

$$0 = \int_{\mathcal{A}} [\mathbf{K}^T(\boldsymbol{\theta}) \mathbf{D}_B \mathbf{K}(\delta \boldsymbol{\theta})] dA + \int_{\mathcal{A}} [\mathbf{S}^T \mathbf{e} \delta \boldsymbol{\theta}] dA + \delta_\theta \Pi_e \tag{19}$$

$$0 = - \int_{\mathcal{A}} [\mathbf{S}^T \mathbf{D}_S^{-1} \delta \mathbf{S}] dA + \int_{\mathcal{A}} [(\nabla w + \mathbf{e} \boldsymbol{\theta})^T \delta \mathbf{S}] dA \tag{20}$$

$$0 = \int_A \{ p - [p - k_x(w - g)]^- \} \delta p \, dA \quad (21)$$

$$0 = \int_{\partial_2 A} [r - (r - k_\beta w)^-] \delta r \, ds \quad (22)$$

where in equation (18) the terms  $[p - k_x(w - g)]^-$  and  $(r - k_\beta w)^-$  can be regarded as Lagrange multipliers.

In Reference 10 Simo and Laursen present an alternative augmented formulation. They augment the functional (12) only through the penalty term, as proposed in Reference 7 for the case of linear constraint. Finally, Simo and Laursen obtain

$$\hat{\Lambda}_{\text{aug}}(w, \boldsymbol{\theta}, \mathbf{S}, r, p) = \Lambda(w, \boldsymbol{\theta}, \mathbf{S}, r, p) + \frac{k_x}{2} \int_A [(w - g)^+]^2 \, dA + \frac{k_\beta}{2} \int_{\partial_2 A} (w^+)^2 \, ds \quad (23)$$

The stationary conditions for the functional (23) lead to equations similar to (18)–(22).

Note that the Lagrangian and the two augmented Lagrangians presented are equivalent; in fact, they admit the same solution state. However, the two augmented Lagrangians allow to develop two different iterative solution algorithms. In particular, when the augmented Lagrangian (17) is exploited, the  $n$ th step of the iterative procedures can be summarized as follows:

- (i) assume the pressures,  $p_{n-1}$  and  $r_{n-1}$ , as known and solve the non-linear equations (18)–(20) in terms of  $w$ ,  $\boldsymbol{\theta}$  and  $\mathbf{S}$ ;
- (ii) update the pressures

$$p_n = [p_{n-1} - \sigma_x(w_n - g)]^-$$

$$r_n = (r_{n-1} - \sigma_\beta w_n)^-$$

with  $\sigma_x > 0$  and  $\sigma_\beta > 0$ ;

- (iii) go to step (i).

The parameters  $\sigma_x$  and  $\sigma_\beta$  used in the pressure update formulas can be chosen independently from the penalty  $k_x$  and  $k_\beta$ .

The algorithm relative to the augmented Lagrangian (23) differs only in the update formulas of the pressures:

$$p_n = p_{n-1} - \sigma_x(w_n - g)^+$$

$$r_n = r_{n-1} - \sigma_\beta w_n^+$$

Both the algorithms return the penalty method at the first iteration; hence, they can be interpreted as iterative penalty methods, with a progressive update of the pressures in order to better satisfy the constraints. Therefore, they can be seen as variants of the procedure proposed by Uzawa.<sup>7</sup>

#### 4. FINITE-ELEMENT FORMULATION

In this section the finite-element implementation relative to the algorithm associated with the augmented Lagrangian (17) is developed; the implementation relative to the augmented Lagrangian (23) is analogous. The domain  $\mathcal{A}$  is discretized using isoparametric finite-elements.<sup>22, 30</sup> Hence,

the typical point in each element is located by the vector  $\mathbf{x} = \{x, y\}^T$  expressed as

$$\mathbf{x} = \sum_{i=1}^{N_{ep}} N^i(\xi, \eta) \hat{\mathbf{x}}^i \tag{24}$$

where  $N_{ep}$  is the number of nodes per element,  $\xi$  and  $\eta$  are the natural co-ordinates of the parent domain,  $N^i$  the shape functions and  $\hat{\mathbf{x}}^i$  the nodal co-ordinates.

A standard displacement-based approach and a linked displacement-rotation-based approach are considered. In both cases only  $C^0$  interpolation functions are adopted.

4.1. A standard displacement-based approach

Displacement-based elements can be obtained from the variational equations (18) and (19) by enforcing the constitutive equation  $\mathbf{S} = \mathbf{D}_S \boldsymbol{\Gamma}$ . At the element level the transverse displacement and the rotations are approximated as

$$\mathbf{w} = \sum_{i=1}^{N_{ep}} N^i \hat{\mathbf{w}}^i, \quad \boldsymbol{\theta} = \sum_{i=1}^{N_{ep}} N^i \hat{\boldsymbol{\theta}}^i \tag{25}$$

indicating with  $\hat{\mathbf{w}}^i$  and  $\hat{\boldsymbol{\theta}}^i = \{\hat{\theta}_x^i, \hat{\theta}_y^i\}^T$  the nodal parameters.

By setting  $N_{ep} = 4$  and  $N_{ep} = 9$ , the so-called Q4 and Q9 plate elements<sup>23, 21</sup> are obtained together with their compatible gap elements. To avoid locking effects, a selective integration formula is adopted to compute the plate stiffness matrix. On the other hand, the reduced integration on the shear terms introduces free energy modes, as discussed in References 22 and 24.

4.2. A linked approach

Linked field and boundary gap elements, compatible with the locking-free four-node plate element Q4-LIM proposed in Reference 25, are obtained by discretizing equations (18)–(20). The transverse displacement interpolation is taken bilinear in the nodal parameters  $\hat{\mathbf{w}}^i$ , enriched with linked quadratic functions of the nodal rotations:

$$\mathbf{w} = \sum_{i=1}^4 N^i \hat{\mathbf{w}}^i - \sum_{i=1}^4 N_{w\theta}^i L^i (\hat{\theta}_n^j - \hat{\theta}_n^i) \tag{26}$$

where  $L^i$  is the  $i$ - $j$  side length,  $\hat{\theta}_n^i$  and  $\hat{\theta}_n^j$  are the components of the rotations of  $i$  and  $j$  nodes in the direction normal to the  $i$ - $j$  side. The  $N_{w\theta}^i$  shape functions are:

$$\mathbf{N}_{w\theta} = \begin{Bmatrix} N_{w\theta}^1 \\ N_{w\theta}^2 \\ N_{w\theta}^3 \\ N_{w\theta}^4 \end{Bmatrix} = \frac{1}{16} \begin{Bmatrix} (1 - \xi^2)(1 - \eta) \\ (1 + \xi)(1 - \eta^2) \\ (1 - \xi^2)(1 + \eta) \\ (1 - \xi)(1 - \eta^2) \end{Bmatrix} \tag{27}$$

Because of the linked interpolations, both the transverse displacement and the rotations contribute to define the gap stiffness matrix and pressure vector. For the plate element, the interpolation for the rotational field is bilinear in the nodal parameters  $\hat{\boldsymbol{\theta}}^i$ , with added internal degrees of freedom.

### 4.3. Numerical integration

Within the finite-element method numerical integrations are often performed through the classical Gauss technique. However, in contact problems the functions to integrate for the computation of the stiffness can be discontinuous in the domain of integration. This discontinuity renders the Gauss scheme unable to perform accurate integral evaluation; common remedies are the use of a large number of integration Gauss points or a very fine mesh. While the first remedy is not completely satisfactory, the second is computationally too expansive also because the contact no-contact zone is not known *a priori*; hence, the mesh should be uniformly fine. On the other hand, a satisfactory computation of integrals for discontinuous functions can be obtained by using the Simpson method with a fine discretization of the domain of integration.<sup>20, 31</sup> This integration technique is more accurate but at the same time is computationally more CPU time-consuming than Gauss integration rule.

For contact problems the functions to be integrated not only are discontinuous but they are non-zero only on the contact zone. This allows the development of a new integration strategy, which is accurate and efficient at the same time. The algorithm is based on the concepts of no-contact, partial contact and full contact. In order to develop a simple procedure, it is assumed that an element is in no-contact if none of the nodes is in contact; it is in partial contact if at least one node is in contact and one node is not in contact. Finally, an element is in full contact when all the nodes are in contact. Hence, the contact state is assumed to be determined by nodal quantities. The details of the integration algorithm are as follows. For a given element the state of contact is determined. If the element is in no-contact, then no integration is necessary. If the element is in full contact, then the Gauss scheme is used for the integration. If the element is in partial contact, then the zone of contact is individuated and a Simpson method is adopted only on the region in contact.

For a field gap in partial contact with the rigid support, the contact zone is determined computing the two points on the sides of the element where the pressure goes to zero and connecting them by a straight line. Hence, the contact zone is approximated to a polygon with 3, 4 or 5 sides. Then, a discretization of the assumed contact zone is performed and the Simpson integration rule is used.

### 4.4. Computational remarks

The finite-element implementation of the presented augmented Lagrangian formulations leads to non-linear algebraical problems. The algorithms consist in a double iterative loop: an external loop for the augmentation, an internal one for the solution of the non-linearity (for example, through the Newton–Raphson method). In particular, the algorithm relative to the formulation (17) is:

- Augmentation DO loop n:
  - Newton–Raphson
    - DO loop i:

$$\begin{aligned}
 \mathbf{A}(\mathbf{U}_n^{i-1})\Delta\mathbf{U}_n^i &= \mathbf{K}\Delta\mathbf{U}_n^i + k_\alpha\mathbf{Q}^\alpha(\mathbf{U}_n^{i-1})\Delta\mathbf{U}_n^i + k_\beta\mathbf{Q}^\beta(\mathbf{U}_n^{i-1})\Delta\mathbf{U}_n^i \\
 &= \mathbf{F} + \mathbf{P}_{n-1} + \mathbf{R}_{n-1} \\
 \mathbf{U}_n^i &= \mathbf{U}_n^{i-1} + \Delta\mathbf{U}_n^i
 \end{aligned} \tag{28}$$

- next i;

– Pressure update:

$$\mathbf{P}_n = \langle \mathbf{P}_{n-1} - \sigma_x (\mathbf{U}_n - \mathbf{G}) \rangle \tag{29}$$

$$\mathbf{R}_n = \langle \mathbf{R}_{n-1} - \sigma_\beta \mathbf{U}^n \rangle \tag{30}$$

◦ next n;

where  $\mathbf{A}(\mathbf{U}_n^{i-1})$  is the global tangent matrix,  $\mathbf{K}$  is the plate stiffness matrix,  $\mathbf{Q}^\alpha(\mathbf{U}_n^{i-1})$  and  $\mathbf{Q}^\beta(\mathbf{U}_n^{i-1})$  are the penalty tangent matrices,  $\mathbf{U}_n$  collects all the nodal displacements,  $\mathbf{F}$  is the force vector,  $\mathbf{P}_n$  and  $\mathbf{R}_n$  are the pressure vectors,  $\mathbf{G}$  is the gap vector, and the symbol  $\langle \bullet \rangle$  is the operator which selects in a vector the negative part of each component corresponding to the transversal displacement degree of freedom. At the  $i$ th iteration of the  $n$ th non-linear problem the test for detecting the field contact is

$$\text{if } [p_{n-1} - k_x(w_n^{i-1} - g) < 0] \text{ then there is contact}$$

An analogous test must be performed for the edge contact.

A crucial point for the convergence of the whole algorithm is the choice of the parameters  $k_x$ ,  $k_\beta$ ,  $\sigma_x$  and  $\sigma_\beta$ . As previously pointed out,  $k_x$  and  $k_\beta$  play the role of penalty parameters. Therefore, a rational choice of these should pass through the evaluation of the condition number  $\kappa(\mathbf{A})$  of the global tangent matrix. However,  $\kappa(\mathbf{A})$  cannot be evaluated *a priori*: in fact, due to the problem non-linearity, the tangent matrix changes at each iteration. Nevertheless, it is possible to perform some considerations, leading to an estimation of  $\kappa(\mathbf{A})$ .

To this end, the symbolic manipulator code Maple<sup>32</sup> is used to determine the expression of a typical stiffness matrix for a Q4-LIM element and for a field and a boundary gap element as a function of the element size, thickness, Young's modulus and penalty coefficient. The study is limited to the case  $\nu = 0.3$  and square geometry with length side  $l_e$ . Characteristic terms of the stiffness matrix for the evaluation of  $\kappa(\mathbf{A})$  are

$$A_{ww}^{e(pl)} = \frac{Eh^3}{\omega} \frac{169}{15000} h^4 + \frac{335}{1064201} h^2 l_e^2 + \frac{136}{61876373} l_e^4$$

$$A_{\theta\theta}^{e(pl)} = Eh^3 \left[ \frac{3772}{96179} + \frac{l_e^2}{\omega} \left( \frac{987}{631208} h^4 + \frac{447}{11274883} h^2 l_e^2 + \frac{73}{263815247} l_e^4 \right) \right]$$

$$A_{w\theta}^{e(pl)} = \frac{Eh^3 l_e}{\omega} \left( \frac{983}{271089} h^4 + \frac{234}{2383075} h^2 l_e^2 + \frac{23}{34702006} l_e^4 \right)$$

$$A_{ww}^{e(b-gap)} = \frac{1}{3} k_\beta l_e, \quad A_{ww}^{e(f-gap)} = \frac{1}{9} k_x l_e^2$$

$$A_{\theta\theta}^{e(b-gap)} = \frac{1}{120} k_\beta l_e^3, \quad A_{\theta\theta}^{e(f-gap)} = \frac{1}{360} k_x l_e^4$$

$$A_{w\theta}^{e(b-gap)} = \frac{1}{24} k_\beta l_e^2, \quad A_{w\theta}^{e(f-gap)} = \frac{1}{12} k_x l_e^3$$

where

$$\omega = \left( \frac{39}{50} h^2 + \frac{91}{4608} l_e^2 \right) \left( \frac{169}{2500} h^4 + \frac{872}{536039} h^2 l_e^2 + \frac{19}{2009616} l_e^4 \right)$$

and the superscripts pl, b-gap and f-gap indicate quantities relative to the plate, the boundary gap and the field gap, respectively. An approximated evaluation of the influence of the penalty

parameters  $k_x$  and  $k_\beta$  on the conditioning of the stiffness matrix of the structure can be performed by considering a submatrix  $\mathbf{A}^{\text{sub}}$  of  $\mathbf{A}$  defined as

$$\mathbf{A}^{\text{sub}} = \begin{bmatrix} A_{ww}^{e(\text{pl})} & A_{w\theta}^{e(\text{pl})} & 0 & 0 \\ A_{w\theta}^{e(\text{pl})} & A_{\theta\theta}^{e(\text{pl})} & 0 & 0 \\ 0 & 0 & A_{ww}^{e(\text{pl})} + A_{ww}^{e(\text{gap})} & A_{w\theta}^{e(\text{pl})} + A_{w\theta}^{e(\text{gap})} \\ 0 & 0 & A_{w\theta}^{e(\text{pl})} + A_{w\theta}^{e(\text{gap})} & A_{\theta\theta}^{e(\text{pl})} + A_{\theta\theta}^{e(\text{gap})} \end{bmatrix}$$

where the superscript *gap* now indicates either the boundary or the field gap. The condition number  $\kappa(\mathbf{A}^{\text{sub}})$  should be compatible with the computer precision.

The choice of the update parameters  $\sigma_x$  and  $\sigma_\beta$  is related to conditions which ensure the convergence to the solution of the perfectly constrained problem. In fact, when the functional (17) is considered, the convergence is guaranteed at least for  $\sigma_x = k_x$  and  $\sigma_\beta = k_\beta$ .<sup>29</sup> When the functional (23) is considered, the convergence is proved for  $0 < \sigma_x < 2k_x$  and  $0 < \sigma_\beta < 2k_\beta$  only in the case of linear constraints.<sup>7</sup>

Several different schemes relative to the choice of  $k_x$ ,  $k_\beta$ ,  $\sigma_x$  and  $\sigma_\beta$  are possible. In the following only two possibilities are investigated:

- (a)  $\sigma_x = k_x$  and  $\sigma_\beta = k_\beta$ , constant during the solution process;
- (b)  $\sigma_x = k_x$  and  $\sigma_\beta = k_\beta$ , increasing during the solution process.

## 5. NUMERICAL EXAMPLES

In this section the inadequacy of the displacement-based elements for the study of contact problems is initially shown. Then, the performances of algorithms based on the augmented Lagrangian formulations previously described are investigated.

The solution algorithm and the finite-elements considered are implemented in the Finite Element Analysis Program (FEAP).<sup>30</sup>

### 5.1. Comparison between plate elements

A simply supported square plate of side  $L$ , subjected to a pointwise force  $F$  applied at the centre, is considered. The bilateral boundary conditions are imposed using the penalty method; the following non-dimensional parameters are adopted:

$$\frac{h}{L} = 0.01, \quad \frac{FL}{D} = 0.4, \quad \nu = 0.3$$

The computations are performed using the elements Q4, Q9 (with both selective and full integration formulas) and Q4-LIM. Due to the symmetry, only a quarter of the plate is considered (Figure 1). A regular  $16 \times 16$  mesh is used for the analyses with four node elements, while a  $8 \times 8$  mesh is used with the nine-node element.

In Figure 2 the vertical displacements along the boundary ( $x = L/2$  and  $y \in [0, L/2]$ ) are plotted when  $k_\beta h^3/D = 10^{-3}$ . If the selective integration scheme is used with Q4 or Q9, the displacements along the penalty supported edge have the shape of a wave, which has no physical evidence. This result can be interpreted as a direct consequence of the zero-energy modes, present in the displacement-based elements when reduced integration formulas are used on the shear terms of the stiffness matrix. Such a behaviour does not depend on the value of the penalty parameter: in fact, increasing  $k_\beta$ , the amplitude of the displacements along the boundary decreases, but they

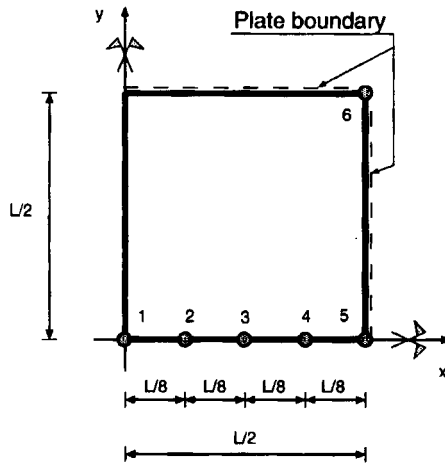


Figure 1. A quarter of square plate. The points of interest are explicitly indicated

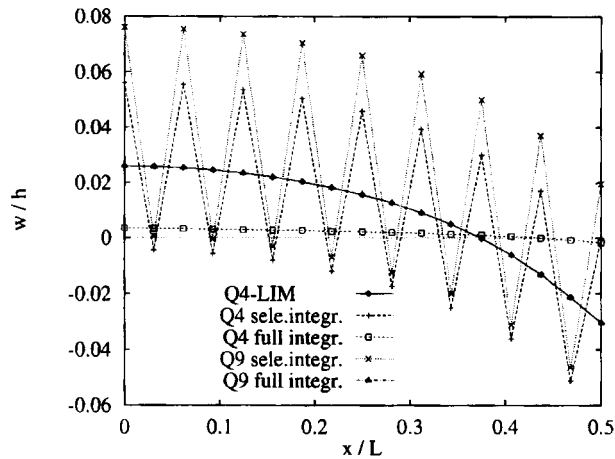


Figure 2. Plate on bilateral supports enforced through penalty method. Displacement along the boundary

still form a wave. As a consequence, within either the penalty or the augmented formulations, a state of contact no-contact, again in the form of a wave, is induced, making it impossible to reach a converged solution.

On the other hand, if full integration formulas are used, the Q4 and Q9 elements do not produce anymore the wave along the boundary. However, they suffer locking as discussed in the literature.<sup>23, 24</sup> On the contrary, the Q4-LIM element is locking-free,<sup>25</sup> and it does not present any wave along the boundary.

From the previous considerations, it can be concluded that the two displacement-based elements are not appropriate for the analysis of plate contact problems within the discussed penalty and augmented Lagrangian formulations; hence, in the remaining examples only the Q4-LIM plate element and its compatible gap elements are used.

5.2. Cylindrical bending of strip plates

A set of simple problems, consisting in strip plates under cylindrical bending, is investigated. Analytical solutions carried out using the Kirchhoff-Love plate theory are compared with FE solutions obtained neglecting the shear energy as described in Reference 25. The plate has unit base, length  $L$  and it is subjected to a constant distributed load,  $q$ . The  $x$ -co-ordinate is taken in the direction of the length; due to the cylindrical bending, in the following all the quantities are expressed only as functions of  $x$  and the symbol ' indicates a derivative along  $x$ .

As a first didactic example, a plate clamped at  $x = 0$  (i.e.  $w(0) = 0$  and  $\theta_y(0) = w'(0) = 0$ ) and unilaterally supported (through the augmented procedure) at  $x = L$  is considered. Adopting the iteration procedure obtained from the functional (17), the solution after  $n$  augmentations is

$$w_n(L) = \frac{3qL}{8k_\beta(\mu + 1)} \left( \frac{\mu}{1 + \mu} \right)^{n-1}$$

$$r_n(L) = -\frac{3qL}{8} \left[ 1 + \left( \frac{\mu}{1 + \mu} \right)^n \right]$$

with  $\mu = 3D/k_\beta L^3$ . Note that

$$\lim_{n \rightarrow \infty} w_n(L) = 0, \quad \lim_{n \rightarrow \infty} r_n(L) = -\frac{3qL}{8}$$

i.e. the augmented solution converges to the exact solution with the rate of the geometrical series. On the contrary, when the algorithm relative to the functional (23) is used, the convergence to the exact solution is not guaranteed. In fact, it is a simple matter to verify that the iterative procedure stops after only two augmentations without converging to the solution, if the condition  $(\mu - 1)(8 - \hat{q}) < 0$ , with  $\hat{q} = qL^4/Dg$ , is satisfied.

Finite-element solutions are now carried out. The non-dimensional geometric and material parameters are

$$\frac{h}{L} = 0.01, \quad \frac{qL^3}{D} = 10, \quad \nu = 0.0$$

Numerical results relative to two meshes ( $10 \times 1$  and  $100 \times 1$ ) and two penalty parameters ( $k_\beta h^3/D = 10^{-3}$  and  $k_\beta h^3/D = 10^{-5}$ ) are presented in Table I. Note the excellent match between the analytical and the finite-element solution, and the difference in convergence rate as a function of the penalty parameter.

Table I. Clamped-simply supported strip plate: displacement at the support ( $x = L$ ) versus augmentation number. Solution obtained through the augmented Lagrangian formulation

$k_\beta h^3/D$	Augm.#	$w(L)/h$		
		10 elms	100 elms	Analytical
$10^{-3}$	1	3.7358E - 01	3.7389E - 01	3.7388E - 01
	3	3.3579E - 06	3.3444E - 06	3.3481E - 06
	5	6.4655E - 11	3.1064E - 11	2.9907E - 11
$10^{-5}$	1	2.8808E + 01	2.8847E + 01	2.8846E + 01
	3	1.5397E + 00	1.5361E + 00	1.5363E + 00
	5	8.2295E - 02	8.1793E - 02	8.1881E - 02
	30	4.2130E - 10	4.1341E - 10	-7.1054E - 15

Then, a strip plate sliding at  $x = 0$  (i.e.  $w'(0) = w'''(0) = 0$ ) and simply supported at  $x = L$  (i.e.  $w(L) = w''(L) = 0$ ) is considered. The plate lies at a gap distance  $g$  from a rigid support. The exact solution depends on  $\hat{q}$  as follows:

- (a)  $\hat{q} < 24/5 \Rightarrow$  there is no-contact
- (b)  $24/5 \leq \hat{q} \leq 24 \Rightarrow$  the contact occurs only at  $x = 0$
- (c)  $\hat{q} > 24 \Rightarrow$  the contact region is a segment with length  $L_c = (24Dg/q)^{1/4}$

The ratio  $g/h$  is set equal to 3, and two loading cases  $\hat{q}_1 = 5$  and  $\hat{q}_2 = 50$  are considered. The analytical solution of the augmented Lagrangian formulation (17) is determined solving a sequence of differential equations, each one representing a plate in unilateral contact with an elastic Winkler medium. Adopting the iteration procedure obtained from the functional (17), the contact pressure after  $n$  augmentations is

$$p_{n-1} = \left[ -g - k_x \sum_{i=1}^4 (\pi_i^{n-1}(x) e^{\gamma_i x}) \right]^-$$

where  $\gamma_i^4 = -k_x/D$ ,  $\pi_i^{n-1}(x)$  is an  $(n-1)$ th degree polynomial and  $C_i^1$  are constants of integration determined by the boundary conditions. Hence, along the part of plate in contact with the rigid support, the solution is

$$w_n(x) = g - k_x \sum_{i=1}^4 \tilde{\pi}_i^{n-1}(x) e^{\gamma_i x} + \sum_{i=1}^4 [C_i^n e^{\gamma_i x}]$$

with  $\tilde{\pi}_i^{n-1}(x)$  a polynomial of  $(n-1)$ th degree, different from  $\pi_i^{n-1}(x)$ , and  $C_i^n$  are constants of integration determined by the boundary conditions.

The finite-element computations are carried out adopting a  $16 \times 1$  mesh. Initially, the penalty method is used. In Table II the lengths of contact  $L_c/L$  versus the coefficient  $k_x h^4/D$  for both the loading cases are given. Note how the finite-element and the analytical solution are in good agreement for low values of the penalty, which however do not guarantee a good enforcement of the constraints. Increasing the value of the penalty coefficient, a better constraint enforcement can be obtained, at the expense of the number of iterations (not reported here) needed to reach the convergence; in particular, for  $k_x h^4/D > 10^{-3}$  the finite-element method does not converge within 20 iterations.

Table II. Sliding-simply supported strip plate: solution obtained through the penalty formulation. Contact length versus penalty value

$k_x h^4/D$	$L_c/L$			
	Loading case 1		Loading case 2	
	Analytical	FE	Analytical	FE
1E-06	0.103	0.103	0.650	0.647
1E-05	0.053	0.053	0.450	0.424
1E-04	0.025	0.037	0.308	0.307
1E-03	0.012	—	0.250	0.249
Exact sol.	0.000	—	0.167	—

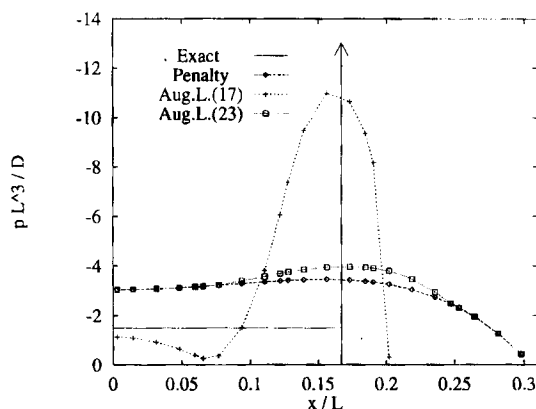


Figure 3. Sliding-simply supported beam seating at a fixed gap distance from a rigid support: ( $\hat{q} = 50$  and  $k_x h^4/D = 1E - 04$ ). Contact pressure along the strip-plate axis: comparison between exact solution, penalty solution and solutions obtained after 200 augmentations from the two augmented Lagrangian procedures considered

Table III. Sliding-simply supported strip plate: solution obtained through the augmented Lagrangian formulation. Contact length versus augmentation number ( $k_x h^4/D = 1E - 04$ )

Augm.#	$L_c/L$			
	Loading case 1		Loading case 2	
	Analytical	FE	Analytical	FE
1	0.025	0.037	0.308	0.307
3	0.017	0.020	0.276	0.276
5	0.014	0.016	0.262	0.265
200		0.003		0.202
Exact sol.	0.000		0.167	

Then, the penalty parameter is set as  $k_x h^4/D = 10^{-4}$ , and the capacity of the augmented Lagrangian formulations (17) and (23) to enforce the constraints is studied. The dimensionless contact pressure  $pL^3/D$  along the strip plate axis is plotted in Figure 5.2 for the loading case  $\hat{q}_2$ ; in particular, the pressure obtained by the penalty solution, and those carried out after 200 augmentations of the two formulations (17) and (23) are reported. The exact solution, consisting in the constant function  $p = q_2$  for  $0 \leq x < L_c$  and in a pointwise force at  $x = L_c$ , is also reported. The convergence of the pressure obtained using the formulation (17) to the exact solution is noted. On the contrary, the solution given by the formulation (23) does not converge to the exact solution; in fact after the first few augmentations the solution does not change and, in terms of pressure, is the one reported in Figure 5.2. In Table III the contact lengths obtained by the analytical and numerical approaches, via augmented formulation (17), are tabulated versus the number of augmentations and are compared with the exact solution. From the results presented, it is possible to conclude that the iterative algorithm relative to the augmented formulation (23) is not appropriate for the solution of contact problems. Hence, only the iterative algorithm relative to the augmented formulation (17) is explored in the remaining examples.

Table IV. Edge contact plate problem: bilateral supports enforced through penalty formulation. Vertical displacement of three significant points versus penalty parameter

$k_\beta h^3/D$	$w_1/h$	$w_5/h$	$w_6/h$
1E-05	5.0818E-01	2.5934E-02	-3.0322E-02
1E-03	4.6737E-01	2.5430E-04	-1.2824E-03
1E-01	4.6654E-01	-2.4141E-06	-1.6959E-05
1E+01	4.6635E-01	-4.3254E-06	-1.2796E-07
1E+03	4.6460E-01	-4.5438E-07	-2.9324E-08
1E+05	4.6438E-01	-5.0568E-09	-3.3021E-10

Table V. Edge contact plate problem: unilateral supports enforced through penalty formulation. Vertical displacement of three significant points versus penalty parameter

$k_\beta h^3/D$	$w_1/h$	$w_5/h$	$w_6/h$
1E-05	1.6905E+00	1.1493E+00	7.4574E-01
1E-03	5.4563E-01	3.0821E-02	-1.5228E-01

### 5.3. Edge contact plate problems

The plate considered in Section 5.1 is discretized by means of  $16 \times 16$  Q4-LIM elements. Initially, both the cases of bilateral and unilateral boundary supports, enforced through the penalty approach, are analysed. The displacement of three points of interest (points 1, 5 and 6 in Figure 1) are reported in Tables IV and V for different values of the non-dimensional penalty parameter  $k_\beta h^3/D$ .

For the case of bilateral supports the problem can be solved for a wide range of the penalty parameter; for high values of such a parameter a good enforcement of the constraint is obtained. On the other hand, the unilateral problem can be solved only for much lower values of the penalty parameter, to which a satisfactory enforcement of the constraints does not correspond. In fact, in Table V  $w_1$  and  $w_5$  have the same order of magnitude, while at the solution it should be  $w_5/w_1 \approx 0$ . Recalling the discussion in Section 4.4,  $\kappa(\mathbf{A}^{\text{sub}})$  can be computed to get an estimate of the problem conditioning. In the case of bilateral constraints  $k_\beta h^3/D|_{\text{max}} = 10^5$  and  $\kappa^b(\mathbf{A}^{\text{sub}}) = 10^6$ ; for the case of unilateral constraints  $k_\beta h^3/D|_{\text{max}} = 10^{-3}$  and  $\kappa^u(\mathbf{A}^{\text{sub}}) = 10$ . Then, it is possible to conclude that the evaluation of the maximum penalty parameter through the condition number  $\kappa(\mathbf{A}^{\text{sub}})$  is indicative only for linear problems. In the case of non-linear problems, the conditions which govern the choice of the penalty parameters are much more restrictive and they are mainly associated with the notion of radius of convergence for a non-linear problem. However, also for the case of non-linear problems, the evaluation of  $\kappa(\mathbf{A}^{\text{sub}})$  gives an upper bound for the penalty parameter to be used during the augmented procedure.

The case of unilateral support is then studied through the augmented Lagrangian formulation (17), setting  $k_\beta h^3/D = 10^{-3}$ . The solutions in terms of the transverse displacements  $w_1$ ,  $w_5$  and  $w_6$  are given in Table VI. A good enforcement of the constraints can be obtained increasing progressively  $k_\beta$  and  $\sigma_\beta$  with  $\sigma_\beta = k_\beta$  and  $\sigma_\beta = 10 * \sigma_\beta$  every three augmentations. During the procedure the penalty parameter never exceeds the upper bound computed through  $\kappa^b(\mathbf{A}^{\text{sub}})$ . The reason for such an increment of the performances can be interpreted as follows: the starting low penalty value allows to solve the unilateral problem and to obtain a qualitative solution of the non-linear problem. Then, the penalty parameter can be progressively increased, inducing a better enforcement of the constraints.

Table VI. Edge contact plate problem: unilateral supports enforced through augmented Lagrangian formulation. Vertical displacement of three significant points versus augmentation number

$k_\beta h^3/D$	Augm.#	$w_1/h$	$w_5/h$	$w_6/h$
1E-3	1	5.4563E-01	3.0821E-02	-1.5228E-01
	4	5.1767E-01	1.7594E-03	-1.5872E-01
	7	5.1658E-01	3.5743E-04	-1.5663E-01
	30	5.1620E-01	-1.7465E-04	-1.5404E-01
1E-3 with update	1	5.4563E-01	3.0821E-02	-1.5228E-01
	4	5.1659E-01	3.3329E-04	-1.5787E-01
	7	5.1616E-01	-4.7225E-05	-1.5405E-01
	30	5.1613E-01	-6.9323E-06	-1.5351E-01

Table VII. Field contact plate problem: unilateral constraint enforced through augmented Lagrangian formulation. Vertical displacement of four significant points versus augmentation number

$k_\beta h^4/D$	$g/h$	Augm.#	$w_1/h$	$w_2/h$	$w_3/h$	$w_4/h$
1E-3	3	1	3.0959E+00	3.1354E+00	3.1368E+00	2.2831E+00
		4	3.0035E+00	2.9960E+00	2.9918E+00	2.2097E+00
		10	3.0042E+00	2.9987E+00	2.9902E+00	2.2124E+00
		30	2.9992E+00	2.9995E+00	2.9876E+00	2.2131E+00
	2	1	2.0916E+00	2.1163E+00	2.1489E+00	1.6476E+00
		4	2.0062E+00	1.9975E+00	2.0097E+00	1.5755E+00
		10	2.0016E+00	1.9996E+00	2.0053E+00	1.5767E+00
		30	1.9993E+00	1.9999E+00	2.0011E+00	1.5767E+00
	1	1	1.0930E+00	1.1032E+00	1.1371E+00	9.4510E-01
		4	1.0049E+00	9.9980E-01	1.0073E+00	8.7146E-01
		10	9.9941E-01	1.0002E+00	1.0019E+00	8.7047E-01
		30	9.9990E-01	1.0002E+00	1.0000E+00	8.7107E-01
1E-3 with update	3	1	3.0959E+00	3.1354E+00	3.1368E+00	2.2831E+00
		4	3.0032E+00	2.9984E+00	2.9912E+00	2.2140E+00
		7	2.9999E+00	3.0000E+00	2.9873E+00	2.2144E+00
		30	3.0000E+00	3.0000E+00	2.9865E+00	2.2145E+00
	2	1	2.0916E+00	2.1163E+00	2.1489E+00	1.6476E+00
		4	2.0023E+00	1.9992E+00	2.0060E+00	1.5785E+00
		7	2.0000E+00	2.0001E+00	2.0004E+00	1.5778E+00
		30	2.0000E+00	2.0000E+00	1.9999E+00	1.5800E+00
	1	1	1.0930E+00	1.1032E+00	1.1371E+00	9.4510E-01
		4	1.0007E+00	1.0001E+00	1.0027E+00	8.7239E-01
		7	1.0000E+00	1.0000E+00	9.9985E-01	8.7137E-01
		30	1.0000E+00	1.0000E+00	9.9998E-01	8.7104E-01

#### 5.4. Field contact plate problems

A plate with the same characteristics of the one previously studied, simply supported along the boundary and subject to a constant distributed load ( $qL^3/D = 100$ ) is considered. The plate seats at a fixed distance  $g$  from a rigid support and the following three cases are considered:

$$\frac{g}{h} \in \{3, 2, 1\}$$

The penalty method is initially adopted. The numerical results, not reported herein for brevity, show that the unilateral field problem can be solved only for low values of the  $k_x h^4/D$  ratio, which give a non-sufficient enforcement of the constraints, as already noted for the edge contact problem. Accordingly, once more the penalty method returns unsatisfactory solutions for a case of unilateral constraints.

The problem is then approached through the augmented Lagrangian formulation (17). In Table VII the vertical displacements of four nodes lying on a symmetry axis (nodes 1, 2, 3 and 4 in Figure 1) are reported. The problem is solved with accuracy if several augmentations are performed while keeping  $\kappa_x$  constant. A good enforcement of the constraint in just few augmentations is obtained by increasing the penalty and the updating parameter, as previously proposed.

## 6. CONCLUSIONS

In the present work unilateral frictionless contact problems within the class of flat structures are studied. The attention is concentrated on two augmented Lagrangian formulations, for which simple solution algorithms can be devised. The implementation within a finite-element scheme is presented and discussed.

For either the penalty or the augmented Lagrangian formulations it is shown that the use of inappropriate plate elements may induce numerical problems. In particular, the pathologies related to the use of Lagrangian isoparametric displacement-based elements are numerically proved.

Accordingly, a more robust linked plate element is adopted. Hence, new field and boundary gap elements compatible with the linked plate element are developed. A computationally efficient technique of integration for the gap elements in partial contact is also proposed. A simple way for estimating the condition number of the global stiffness matrix is presented.

Several numerical examples are considered. Initially, a set of strip plates under cylindrical bending, for which exact solutions are available, are studied; a comparison between exact, analytical and numerical solutions is presented. From such a comparison, it can be concluded that the iterative procedure obtained from one of the augmented Lagrangian formulations considered does not ensure the convergence to the exact solution. More complex unilateral problems, such as a plate constrained through unilateral edge supports and a plate seating in its undeformed configuration at a given distance from a rigid support, are also considered. The numerical results show the effectiveness of the procedure developed, mainly when a progressive increment of the penalty parameters is performed during the augmentations. This technique allows a good enforcement of the constraint and avoids convergence difficulties typical of non-linear contact problems solved through penalty formulations.

## ACKNOWLEDGEMENTS

The authors would like to thank F. Maceri for many useful discussions. Support for the present research was provided by the Italian MURST (Ministero dell' Università e della Ricerca Scientifica) and CNR (Consiglio Nazionale delle Ricerche).

## REFERENCES

1. P. D. Panagiotopoulos, *Inequality Problems in Mechanics and Applications*, Birkhauser, Basel, 1985.
2. G. Romano and E. Sacco, 'Convex problems in structural mechanics', in G. Del Piero and F. Maceri (eds.), *Unilateral Problems in Structural Analysis 3*, CISM Courses and Lectures No. 304, Springer, Berlin, 1987, pp. 279–297.
3. N. Kikuchi and J. T. Oden, *Contact Problems in Elasticity: A Study of Variational Inequalities and Finite Element Methods*, SIAM Studies in Applied Mathematics, 1988.
4. G. Yagawa and Y. Kanto, 'Finite element analysis of contact problems using penalty function method', in M. H. Aliabadi and C. A. Brebbia (eds.), *Computational Methods in Contact Mechanics*, Computational Mechanics Publications, Elsevier Applied Science, 1993.
5. R. Luciano and E. Sacco, 'Stress-penalty method for unilateral contact problems. Mathematical formulation and computational aspect', *European J. Mech. Solids/A*, **13**, 93–112 (1994).
6. D. G. Luenberger, *Linear and Nonlinear Programming*, 2nd edn, Addison-Wesley, Reading, MA, 1989.
7. R. Glowinski and P. Le Tallec, *Augmented Lagrangian and Operator-Splitting Methods in Nonlinear Mechanics*, SIAM Studies in Applied Mathematics, 1989.
8. J. A. Landers and R. L. Taylor, 'An augmented Lagrangian formulation for the finite element solution of contact problems', *Report No. UCBISEMM-85/09*, Department of Civil Engineering, University of California, Berkeley, 1985.
9. P. Alart and A. Curnier, 'A mixed formulation for frictional contact problems prone to Newton like solution methods', *Comput. Methods Appl. Mech. Eng.*, **92**, 353–375 (1991).
10. J. C. Simo and T. A. Laursen, 'An augmented Lagrangian treatment of contact problems involving friction', *Comput. Struct.*, **42**, 97–116 (1992).
11. A. Klarbring, 'Mathematical programming and augmented Lagrangian methods for frictional contact problems', in A. Curnier (ed.), *Proc. Contact Mechanics Int. Symp.*, Presses Polytechniques et Universitaires Romandes, 1992.
12. T. A. Laursen and V. G. Oancea, 'Automation and assessment of augmented Lagrangian algorithms for frictional contact problems', *J. Appl. Mech.*, **26**, 956–963 (1994).
13. G. Zavarise, P. Wriggers and B. A. Schrefler, 'On augmented Lagrangian algorithms for thermomechanical contact problems with friction', *Int. j. numer. methods eng.*, **38**, 2929–2949 (1995).
14. O. J. Svec, 'The unbounded contact problem of a plate on the elastic half space', *Comput. Methods Appl. Mech. Eng.*, **3**, 105–113 (1974).
15. L. Ascione and A. Grimaldi, 'Unilateral contact between a plate and an elastic foundation', *Meccanica*, **19**, 223–233 (1984).
16. D. D. Ang and L. K. Vy, 'Contact of a plate and an elastic body', *Z. Angew. Math. Mech.*, **75**, 115–126 (1995).
17. L. Ascione and G. Bilotti, 'The dynamical problem of an elastic plate resting on a two-parameter foundation which does not react in tension', *Meccanica*, **25**, 92–98 (1990).
18. A. Leonardi and E. Sacco, 'Mechanical behavior of laminates on elastic foundation', *Theoret. Appl. Fract. Mech.*, **16**, 223–235 (1991).
19. R. Lewandowsky and R. Switka, 'Unilateral plate contact with elastic-plastic Winkler-type foundation', *Comput. Struct.*, **39**, 641–651 (1991).
20. E. Barbero, R. Luciano and E. Sacco, 'Three-dimensional plate and contact/friction elements for laminated composite joints', *Comput. Struct.*, **54**, 689–703 (1995).
21. J. N. Reddy, *An Introduction to the Finite Element Method*, 2nd edn, McGraw Hill, New York, 1993.
22. T. J. R. Hughes, *The Finite Element Method*, Prentice-Hall, Englewood Cliffs, N.J., 1987.
23. O. C. Zienkiewicz, R. L. Taylor and J. M. Too, 'Reduced integration techniques in general analysis of plates and shells', *Int. j. numer. methods eng.*, **9**, 275–290 (1971).
24. R. C. Averill and J. N. Reddy, 'Behavior of plate elements based on the first-order shear deformation theory', *Eng. Comput.*, **7**, 57–74 (1990).
25. F. Auricchio and R. L. Taylor, 'A thick plate finite element with exact thin limit', *Comput. Methods Appl. Mech. Eng.*, **3**, 393–412 (1994).
26. P. Bisegna and E. Sacco, 'A rational deduction of plate theories from three-dimensional linear elasticity', *Z. Angew. Math. Mech.*, in press.
27. E. Reissner, 'The effect of the shear deformation on the bending of elastic plates', *J. Appl. Mech.*, **12**, 69–76 (1945).
28. R. D. Mindlin, 'Influence of rotatory inertia and shear in flexural motion of isotropic, elastic plates', *J. Appl. Mech.*, **18**, 31–38 (1951).
29. K. Ito and K. Kunisch, 'An augmented Lagrangian technique for variational inequalities', *Appl. Math. Optim.*, **21**, 223–241 (1990).
30. O. C. Zienkiewicz and R. L. Taylor, *The Finite Element Method*, 4th edn, McGraw Hill, New York, 1991.
31. N. Point and E. Sacco, 'A delamination model for laminated composites', *Int. J. Solids Struct.* (1995).
32. B. W. Char, K. O. Geddes, G. H. Gonnet, B. L. Leong, M. B. Monagan and S. M. Watt, *First Leaves: A Tutorial Introduction to Maple V*, Springer, Berlin, 1992.